

Comparative study of different turbulence modelling approaches to prediction of transonic and supersonic flows past a re-entry capsule with balance flaps

A. Garbaruk, D. Niculin*, M. Strelets*, A. Dyadkin**, A. Krylov**, K. Stekenius****

**St-Petersburg State Polytechnic University*

29, Poytechnicheskaya str., 195251, St-Petersburg, Russia

***RSC "Energia"*

4A, Lenin Street, 141070 Korolev, Moscow region, Russia

****TSNIMASH*

4, Pionerskaya Street, 141070 Korolev, Moscow region, Russia

Abstract

Computations of turbulent flow past a re-entry capsule are carried out with the use of two RANS models and Delayed Detached-Eddy Simulations (DDES) in a wide range of the free stream Mach number ($M_\infty=0.8-6.0$). It is shown that transonic and slightly supersonic mean flow predictions are more sensitive to turbulence treatment than the high Mach number flows. Other than that, DDES reveals significant flow unsteadiness and strong oscillations of forces acting on the capsule which may cause an impact on its survivability. A comparison with experiment on mean flow and integral forces demonstrates a fairly good agreement with the data.

1. Introduction

A reliable CFD prediction of turbulent flows past re-entry vehicles is a challenging physical and numerical problem. This is caused by several factors which include a complexity of geometry, massively separated character of the flow, and its complicated wave pattern. As of today, a number of computational studies of this type of flow is rather limited. Moreover, of them address the hypersonic flow regimes (see, e.g., [1]-[4]), whereas moderately supersonic and transonic flow regimes typical of the approach stage of the flight trajectory and known to be most sensitive to a specific choice of turbulence model are virtually not investigated. Note also that in this stage maneuvering capabilities of a re-entry vehicle become especially important. This motivates systematic numerical studies aimed at evaluating capabilities of the up-to-date turbulence models as applied to exactly these flow regimes. In the present work an attempt is undertaken to address this issue by computing a flow past a re-entry capsule with balance flaps at Mach numbers within the range 0.8-6.0 with the use of three different turbulence modelling approaches (two RANS models and Delayed Detached-Eddy Simulation (DDES) [5] with a primary objective to assess model-sensitivity of major dynamic flow characteristics, first of all, forces and moments acting on the capsule.

The rest of the paper is organised as follows. Section 2 presents a general outline of the computations which includes a description of the capsule geometry, turbulence models used, and computational aspects of the simulations. Then, in Section 3, obtained results are presented and discussed in some detail and in Section 4 a brief description of the experiments is given followed by a comparison of the simulation results with the experimental data.

2. General overview of the computations performed

2.1. Re-entry capsule geometry

Schematics of two considered geometries are shown in Fig. 1. The first one (Fig. 1a) presents a simplified re-entry capsule. It is similar to the capsule investigated in the Fire II experiments (includes a spherical fore-body and an after-body shaped as truncated cone) and, in addition, has a "bulge", where the capsule engines are located, and two balance flaps which differential deflection permits an alteration of the angles of attack and the roll-angle along the trajectory, thus widening capsule's maneuvering capabilities. The capsule diameter, D , is equal to 4.4 m. The second, model, geometry (Fig. 1b) has been investigated in experiments of TSNIMASH (see Section 5). It has the same

shape as the first one but is much smaller ($D_m = 0.075 \text{ m}$) and equipped with a cylindrical support ($d = 0.025 \text{ m}$) aimed at fixing the model in wind-tunnels.

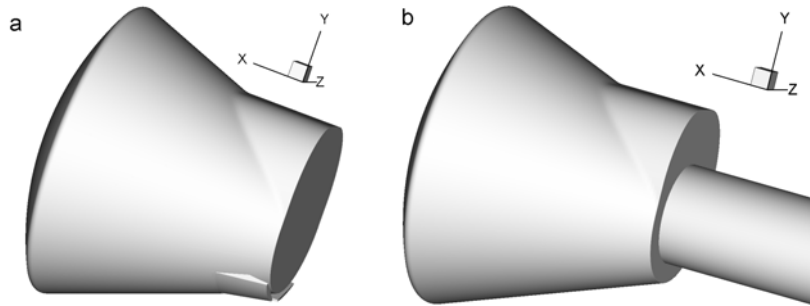


Figure 1: Two considered geometries

2.2. Physical modelling

The air flow past the capsule is assumed to be a compressible flow of the perfect gas with a constant specific heats ratio of 1.4, Prandtl number of 0.71, and molecular viscosity depending on temperature in accordance with the Sutherland law. Considering a primary objective of the study (defining dynamic flow characteristics) and relatively low Mach number (up to 6), these assumptions are quite justified.

As far as turbulence representation is concerned, most of the computations are carried out in the framework of the Reynolds Averaged Navier-Stokes equations (RANS) coupled with the one-equation Spalart-Allmaras model with compressibility correction [6] (SACC model) and two-equation $k-\omega$ Shear Stress Transport model of Menter [7] (SST model), which are currently considered as the most reliable linear RANS models for aerodynamic applications. In addition, some of the computations are conducted with the use of a hybrid RANS-LES approach DDES with the SST background RANS model [5]. DDES presents an enhanced version of the original DES formulation [8] and does not suffer from the so called Modelled Stress Depletion [5] typical of the DES performed on “ambiguous” grids, i.e., the grids with tangential cells sizes less than the boundary layer thickness. This is exactly the case for the considered flow, where fine tangential grids are needed for a correct representation of the geometry and sufficient resolution of the shock waves. Other than that, in order to get an idea on an impact of a laminar flow “patch” on the spherical fore-body of the capsule which exists even at flight conditions corresponding to very high Reynolds numbers, some of the SACC RANS computations have been carried out with the use of two treatments of the laminar turbulent transition. The first one is a conventional fully turbulent (FT) approach, which assumes that the whole boundary layer on the capsule surface is turbulent, whereas within the second (“trip-less” or TL) approach [9], it is supposed that the flow upstream of separation is laminar and transition to turbulence occurs only in the separated shear layer. Implementation of both approaches is briefly discussed in the next section.

2.3. Computational domain, grids, and boundary conditions

A computational domain in all the RANS computations was a half-sphere with the diameter of $40 D$. The domain, its zoomed fragment and a structured multi-block overset grid of Chimera type in the symmetry plane of the capsule are shown in Fig. 2.

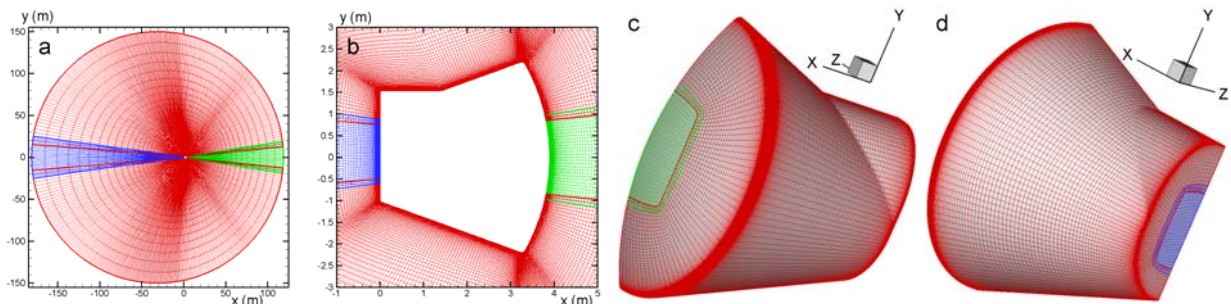


Figure 2: Computational domain (a) and some details of the grid in symmetry plane (b) and on its surface (c and d). The outer (red) grid block is of O-type, and Cartesian-like (blue and green) blocks are introduced to avoid singularity of the governing equations in the vicinity of the capsule axis. The grid is clustered in the wall normal-direction so

that the closest to the wall cell size does not exceed the value of 1 in the wall units ($y_1^+ \leq 1$). Other than that, the grid is refined in the tangential direction in the vicinity of the fore-body / cone and cone / base junctions. A finer resolution in these areas was found to be crucial in the course of preliminary simulations which suggest that otherwise some peculiarities of the flow patterns (local supersonic zones, shocks and rarefaction waves) cannot be properly represented.

For the cases with deflected balance flaps, additional grid blocks are introduced as illustrated by Fig. 3.

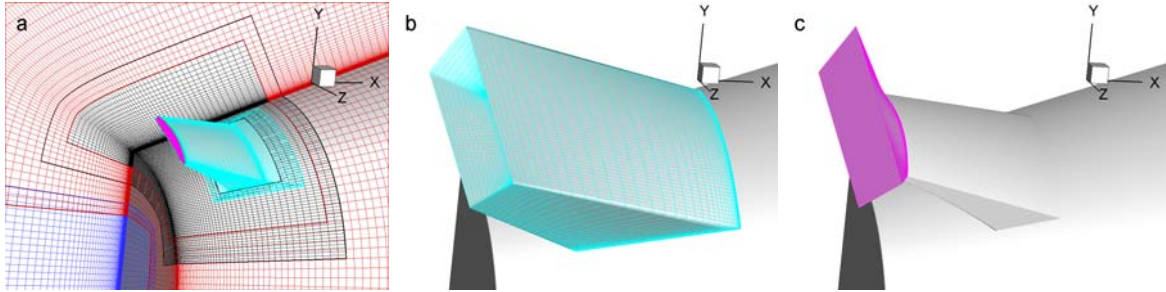


Figure 3: Some elements of the grid for RANS of the capsule with deflected flaps. a: cut-out in the main outer block and flap surface grid; b: flap block; c: flap blunted edge block

Finally, for the capsule with the cylindrical support, an additional grid block of O-type is embedded into the main grid block (blue block in Fig.4).

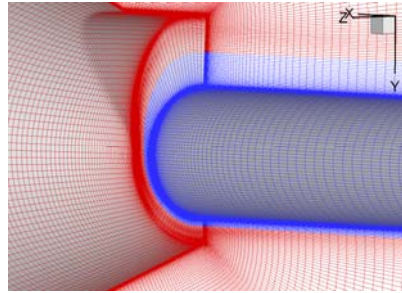


Figure 4: Zoomed grid fragment in the vicinity of the support

As far as the DDES grid is concerned, its topology is the same as that of the grid used for RANS, but the computational domain in this case is a whole sphere rather than a half-sphere (for a turbulence-resolving approach, symmetry assumption is not justified) and the grid in the LES region of DDES is significantly refined compared to that used in RANS (see Fig. 5) in accordance with recommendations [10]. As a result, the grid has about 5 million nodes (typical RANS grids have from 2.3 to 3.0 million nodes).

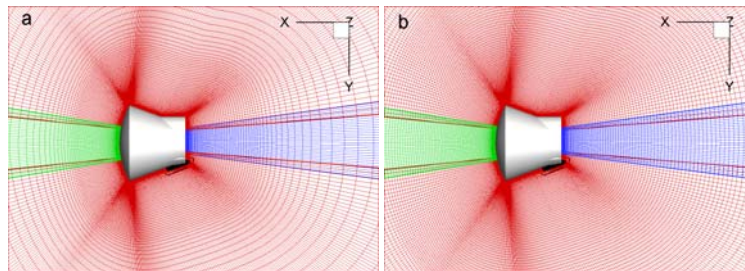


Figure 5: Zoomed fragments of computational grids in the symmetry plane used in RANS (a) and DDES (b)

Boundary conditions in all the computations are imposed as follows.

On the solid walls, non-permeability and no-slip conditions are imposed for the velocity vector ($u_w = v_w = w_w = 0$) and the adiabatic condition for the temperature ($\partial T / \partial n|_w = 0$). The modified eddy viscosity $\tilde{\nu}$ on the wall in the SA model transport equation is set equal to zero, whereas within the SST model the turbulent kinetic energy is set zero and its specific dissipation rate is computed as $\omega_w = 10[6\nu/(\beta_1\Delta y_1^2)]$ [7], where ν is the molecular viscosity, $\beta_1=0.075$ is the constant of the SST model, and Δy_1 is the first near wall grid step.

At the outer boundary of the computational domain, for the aerodynamic variables the characteristic boundary conditions are imposed and the turbulent quantities are defined as follows. For the SACC model, the eddy viscosity at the inflow parts of the outer boundary, $\nu_{t\infty}$, is specified. For the SST model, the inflow value of the specific dissipation rate is defined as [7] $\omega_\infty = CU_\infty / D$ (U_∞ is the free stream velocity and the constant C is within the range 1÷10), whereas the inflow turbulent kinetic energy, k_∞ , is computed via ω_∞ and the eddy viscosity $\nu_{t\infty}$: $k_\infty = \rho_\infty \nu_{t\infty} \omega_\infty$. As far as the specific value of the inflow eddy viscosity is concerned, it depends on the approach used for laminar-turbulent transition control. If the FT approach is used, it is set equal to the molecular viscosity, which is known to provide a rapid forming of the developed turbulent boundary layer on the body surface. In the framework of the TL approach (laminar flow upstream of the separation and turbulent flow in the separated shear layer and separation region), computations are carried out in two stage [9]. In the first stage, the boundary conditions are the same as within the FT approach ($\nu_{t\infty} = \nu$). This computation is performed until forming a recirculation zone in the leeward region of the capsule. After that, the inflow value of the eddy viscosity is set to some small value ($10^{-3}\nu$), and the computation is continued until a converged steady-state solutions is obtained. As a result, the eddy viscosity in the attached boundary layer becomes zero (it is “washed out” by convection) and in the recirculation zone and the wake the flow remains turbulent.

Finally, at the outflow parts of the outer boundary, all the turbulent quantities are defined by the linear extrapolation from the interior of the domain.

2.4. Numerics

All the computations are carried out with the use of the compressible branch of the in-house NTS code [11]. This is a structured multi-block code well established in the field of modern turbulence-resolving treatments. The code has passed extensive code-to-code comparisons with other public, in-house industrial, and commercial CFD codes (CFL3D of NASA, GGNS of Boeing, ELAN of the Technical University of Berlin, CFX and FLUENT) and, as of today, is considered as one of the most reliable and efficient research CFD codes for aerodynamic applications. For compressible flow simulations the code employs an implicit high order hybrid (weighted, 3rd order upwind / 4th order centred) flux difference splitting scheme of Roe [12] with local limiters. Time integration is carried out with second order three-layer scheme and numerical implementation is performed by implicit relaxation algorithms (Plane/Line Gauss-Seidel relaxation and Diagonally Dominant ADI algorithm), which may be arbitrarily specified by a user in different grid-blocks.

2.5. Matrix of cases

With the use of the methodology briefly outlined above, a wide range of computations has been performed for both flight and wind-tunnel conditions at different flow regimes (Mach number, angle of attack, α , and flaps deflection angle, δ_F). However in this paper we focus mostly on a few cases which are most revealing in terms of assessment of different approaches to turbulence modelling. These cases are summarized in Table 1.

Table 1: Matrix of cases

Case	Flight / Wind-Tunnel (WT) Conditions	Altitude, km	Mach number	Reynolds number	$\alpha,^\circ$	$\delta_F,^\circ$	Turbulence treatment	Transition treatment
1	Flight	15	0.8	$1.42 \cdot 10^7$	20	10	SACC RANS	FT
2	Flight	15	0.8	$1.42 \cdot 10^7$	20	10	SST RANS	FT
3	Flight	15	0.8	$1.42 \cdot 10^7$	20	10	SA DDES	FT
4	Flight	40	6.0	$2.09 \cdot 10^6$	20	0	SACC RANS	FT
5	Flight	40	6.0	$2.09 \cdot 10^6$	20	0	SST RANS	FT
6	WT	-	0.8	$1.54 \cdot 10^6$	20	0	SACC RANS	FT
7	WT	-	0.8	$1.54 \cdot 10^6$	20	0	SACC RANS	TL

3 Results and discussion

3.1. Turbulence model and transition control sensitivity

Simulations performed have shown that an impact of turbulence model on predicted mean flow characteristics and integral forces acting on the capsule is most pronounced for the transonic and slightly supersonic flow regimes. This

is illustrated by a comparison of results obtained with the use of three different approaches to turbulence representation at $M=0.8$ (cases 1-3 in Table 1) presented in Fig.6.

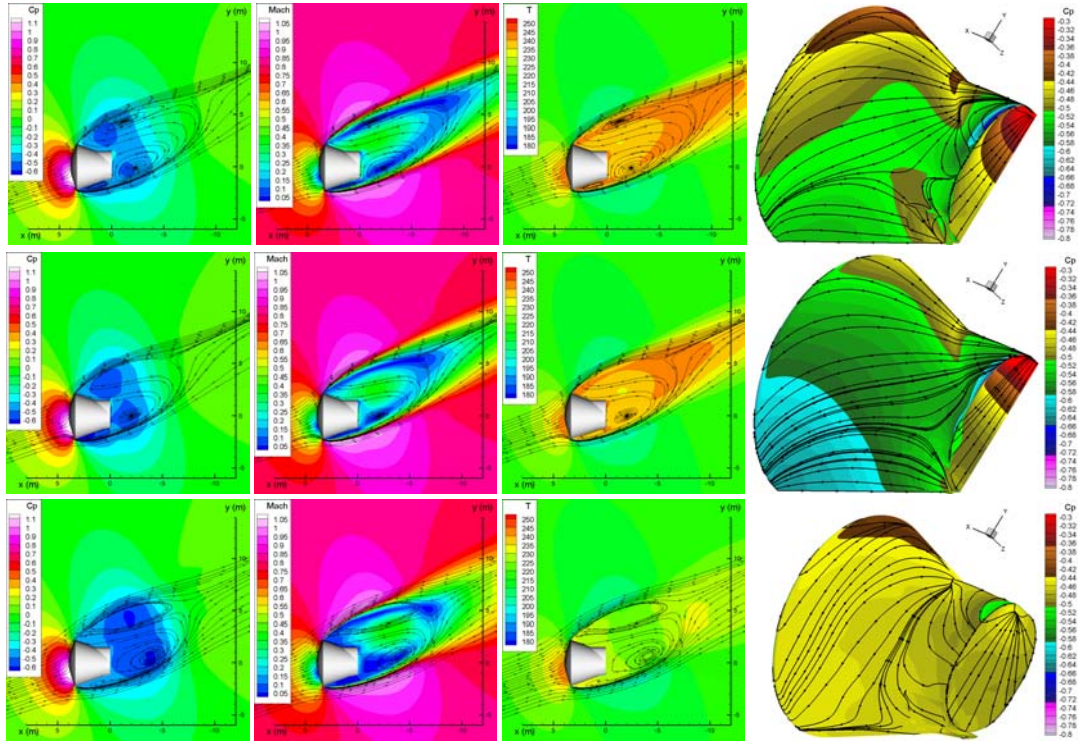


Figure 6: Comparison of streamlines and contours of mean pressure (C_p), Mach number, and temperature (T) in symmetry plane and surface pressure and streamlines (“oil flow”) from SACC RANS (first row), SST RANS (second row), and SA DDES (third row). Cases 1-3 from Table 1

The figure reveals not only a considerable difference between the RANS and DDES predictions (this could be expected for the massively separated flow), but far from identical RANS solutions with the SACC and SST turbulence models. Particularly, the recirculation zone predicted by the SST model is noticeably shorter than that predicted by the SACC model and is close to the DDES prediction. The pressure, Mach number, and temperature fields in the symmetry plane and the surface pressure from the two RANS solutions are also somewhat different but both are far from those predicted by the DDES: the latter are much more uniform. Note that this trend is consistent with that observed in RANS and DES computations of the supersonic base flow [13], [14].

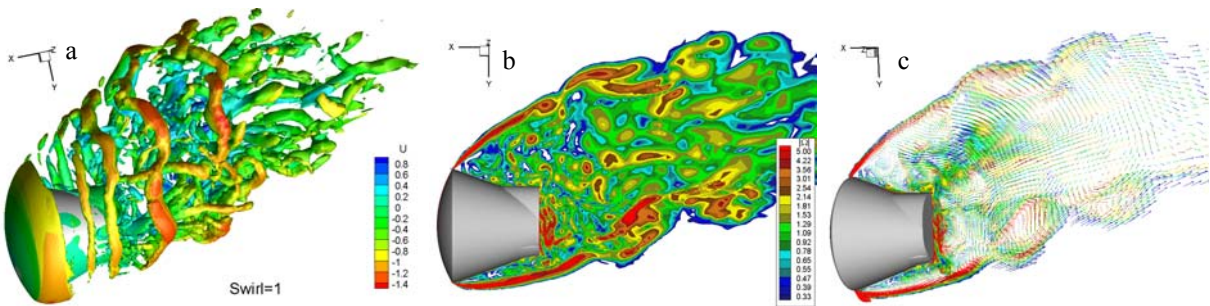


Figure 7: Instantaneous swirl isosurface coloured by streamwise velocity (a), contours of vorticity magnitude in the symmetry plane (b), and velocity vectors in the symmetry plane coloured by vorticity magnitude (c) from DDES of $M=0.8$ flow (Case 3 in Table 1)

A reason of observed differences between the RANS and DDES predictions is a complicated 3D unsteady vortical structure of the wake flow which is characterized by presence of both relatively large vortical rings and streamwise vortices and fine-grained turbulence (see Fig. 7), i. e, by the features that cannot be captured by a RANS model of any level of complexity. As a result, instantaneous integral forces and, especially, moments predicted by the DDES experience strong oscillations (see Fig.8 and Table 2). As far as the mean forces are concerned, their values computed with the use of different turbulence models also turn out to be different but the scatter is not too wide (see Table 2).

In contrast to the transonic flow, at $M=6$, SACC and SST RANS predictions of the flow- and wave-patterns over the capsule turn out to be very close to each other (see Fig.9), which suggests that at the high supersonic and hypersonic flight conditions the effect of turbulence model is insignificant.

Table 2: Effect of turbulent model on integral forces and moments (Cases 1-3 from Table 1)

Case	Turbulence Treatment	C_x	C_y	C_z	C_y/C_x	M_x	M_y	M_z
1	SACC RANS	1,0082	-0,351	0	-0,349	0	0	-0,015
2	SST RANS	1,0394	-0,383	0	-0,369	0	0	-0,014
3	SA DDES	1,0117	-0,309	-0,006	-0,306	-0,0005	-0,004	-0,002

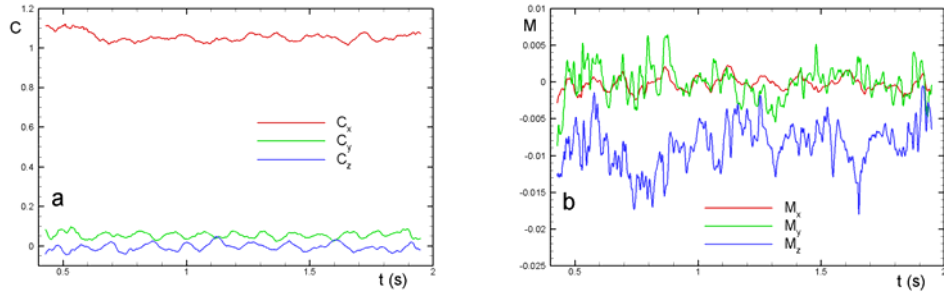


Figure 8: Time variation of coefficients of integral forces (a) and moments (b) from DDES

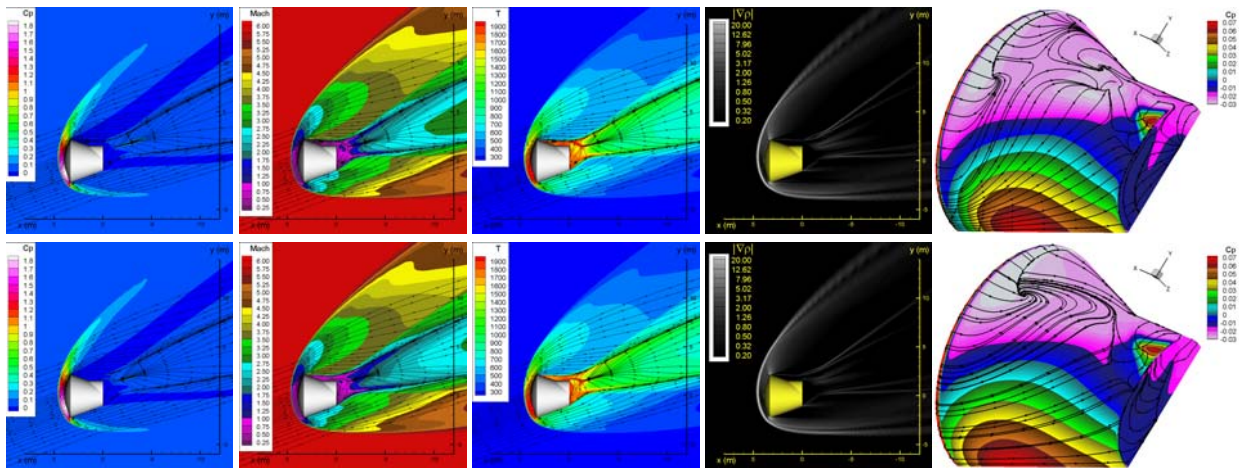


Figure 9: Comparison of streamlines and contours of mean pressure, Mach number, temperature, and magnitude of density gradient (numerical Schlieren) in the symmetry plane and surface pressure and streamlines from SACC RANS (first row) and SST RANS (second row). Cases 4, 5 in Table 1

In addition to the turbulence modelling itself, an important aspect of numerical simulations of the considered flow is a treatment of the laminar-turbulent transition, the more so that due to a significant difference of the Reynolds numbers at flight and WT conditions, the transition process in flight and in experiments may be considerably different. As already mentioned, in order to assess a sensitivity of the predictions to the transition treatment, in the present study two approaches to its control in the simulations have been used, first (FT) assuming a fully turbulent flow past the whole capsule and the second (TL) supposing that the flow upstream of separation is laminar and transition to turbulence occurs in the separated shear layer. A comparison of results obtained with the use of these two approaches at the WT conditions (Cases 6 and 7 from Table 1), i.e., when the flow in the fore-body boundary layer is most likely laminar, is presented in Fig. 10. It shows that in accordance with designs of the TL and FT approaches, in the first case the eddy viscosity shows up only downstream of the separation, whereas in the second case it is non-zero all over the fore-body boundary layer. However, even with the FT approach, due to the strong flow acceleration, the boundary layer remains close to laminar (the eddy viscosity is less than the molecular one). Other than that, the minor difference between the eddy viscosity fields in the fore-body boundary layer does not cause any noticeable alteration of the surface pressure and “CFD oil flow” (surface streamlines) topology (see Fig.10 c, d) Thus, at least for the considered geometry and flow regimes, a more simple FT approach to the transition control seems to be fully justified.

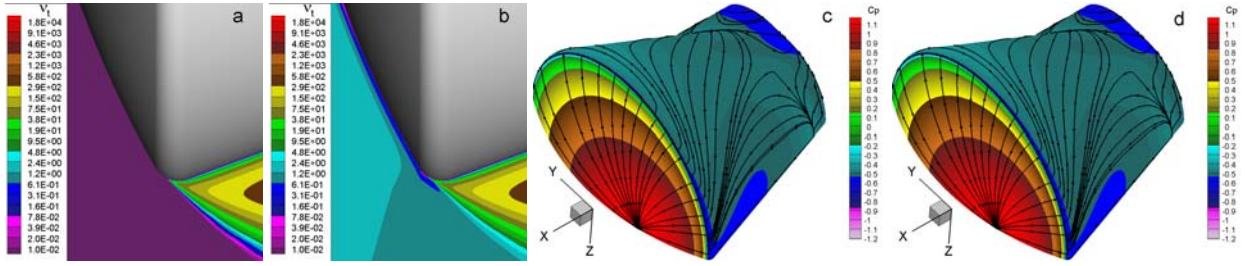


Figure 10 : Zoomed fragments of eddy viscosity from the TL (a) and FT (b) SACC RANS at the $M=0.8$ (Cases 7, 6 in Table 1) and surface pressure distributions and streamlines for the same computations (c, d)

3.2. Comparison with experiment

The experimental study has been carried out in the wind-tunnels U-3M, U-4M and U-303-3 TSNIIMASH for the model geometry (see Fig.1) manufactured by the RKK “Energia”. The Mach number, Reynolds number based on the model diameter, and angle of attack in the experiments varied within the ranges $0.27\div 7.7$, $7.1 \times 10^5 \div 2.7 \times 10^6$, and $0^\circ \div 40^\circ$, respectively. The integral forces and moments acting on the capsule were measured with the use of an internal six-component strain unit with the errors not exceeding ± 0.02 for the drag coefficient, ± 0.01 for the lift coefficient, and ± 0.001 for the z -component of the moment coefficient. In addition, in the course of experiments Schlieren pictures of the flow were made, which permits to analyze its wave-pattern.

Figure 11 compares experimental Schlieren picture with the numerical one (contours of the magnitude of the density gradient) obtained with the use of the SACC turbulence model. The figure suggests that the computation does capture all the details of the flow wave-pattern observed in the experiment. Similar results (not shown) are obtained with the use of the SST RANS and DDES.

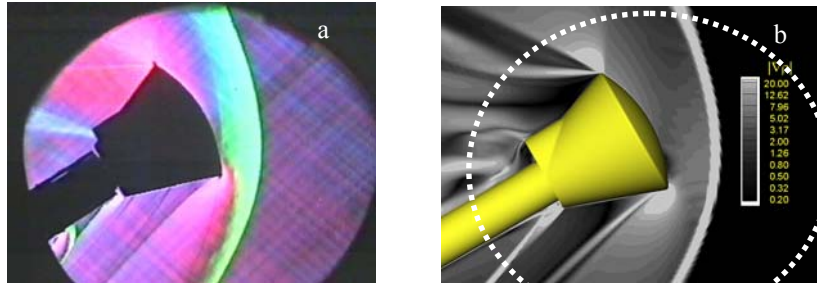


Figure 11: Experimental (a) and numerical (b) Schlieren pictures of the flow $M=1.5$, $Re = 1.9 \cdot 10^6$, and angle of attack 30° . Dashed white line shows experimental window

Finally, Fig. 12 presents a comparison of the measured coefficients of integral forces and moments with those predicted by the different turbulence models for all the considered flow regimes at flight and experimental conditions (for the latter, the computations were performed both with and without the model support). As seen in the figure, all the predictions are well within the range of the experimental uncertainty.

4. Conclusions

RANS (with the SACC and SST turbulence models) and SST-based DDES computations are performed of the re-entry capsule with and without balance flaps. Results obtained reveal a tangible sensitivity of the mean flow predictions to the turbulence modeling approaches at the transonic and slightly supersonic flow regimes and their marginal sensitivity to turbulence model at high Mach numbers ($M=3\div 6$). However, as of today, it is difficult to give a definite preference to any of the considered approaches because of the considerable scatter of the experimental data on the integral forces acting on the capsule and absence of data for other flow parameters. We can state only that all the models are capable of predicting the mean flow characteristics of the flow past the re-entry capsule and the integral forces and moments within the experimental scatter. The DDES approach provides, in addition, valuable information on the unsteady loads on the capsule.

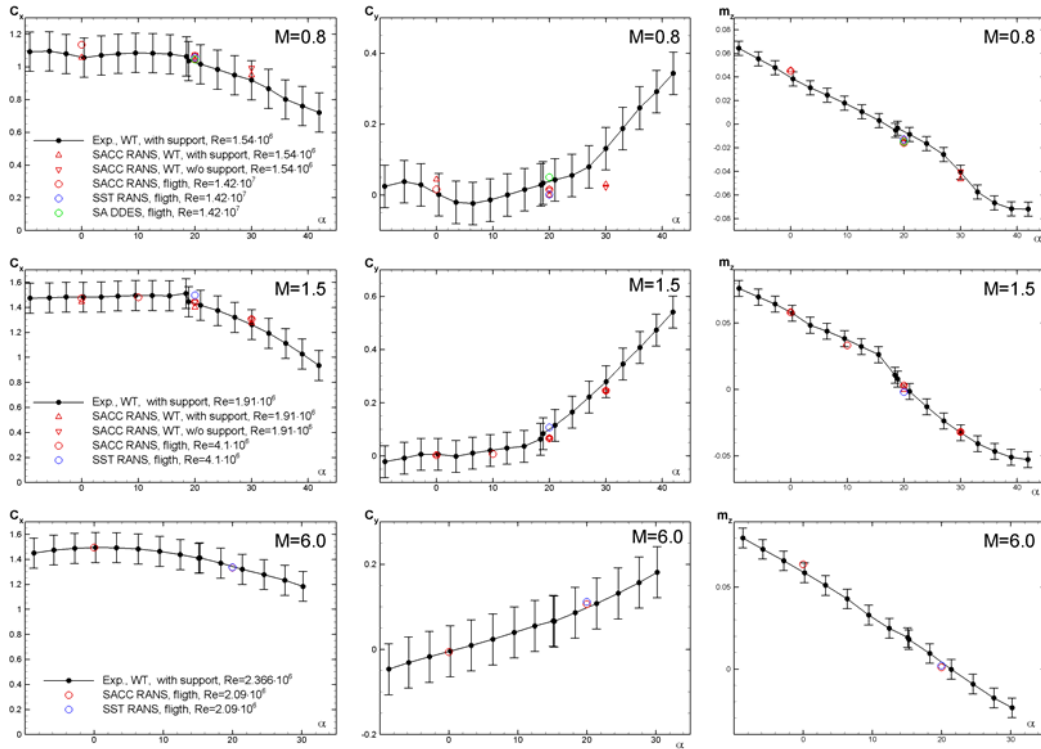


Figure 12: Comparison of predicted and measured coefficients of integral forces and moments

References

- [1] Longo, J.M.A. 2004. Modelling of Hypersonic Flow Phenomena. In: *VKI-RTO Lecture Series "Critical Technologies for Hypersonic Vehicle Development Technology"*, VKI, Belgium. RTO-EN-AVT-116.
- [2] Sinha, K., M. Barnhardt and G.V. Candler. 2004. Detached Eddy Simulation of Hypersonic Base Flows with Application to Fire II Experiments. *AIAA Paper* 2004-2633.
- [3] Kushal S., K. Sinha, 2006. Effect of compressibility corrections to turbulence models applied to a hypersonic re-entry configuration. NCFMFP 2006-1221 In: *Proceedings of 33rd National and 3rd International Conference on Fluid Mechanics and Fluid Power, December 7-9, 2006, II T Bombay India.*
- [4] Sinha, K. and C. Vadivelan. 2008. Effect of Angle of Attack on Re-entry Capsule Afterbody Flowfield. *AIAA Paper*, 2008-1282.
- [5] Spalart P.R., S. Deck, M.L. Shur, K.D. Squires, M.Kh. Strelets and A.K. Travin. A New Version of Detached-Eddy Simulation, Resistant to Ambiguous Grid Densities. *Theor. Comp. Fluid Dyn.* 20:181-195.
- [6] Spalart, P.R. 2000. Trends in Turbulence Treatments. *AIAA Paper* 2000-2306.
- [7] Menter, F.R. 1993. Zonal Two Equation $k-\omega$ Turbulence Models for Aerodynamic Flows. *AIAA Paper* 93-2906.
- [8] Spalart, P.R., W.-H. Jou, M. Strelets, and S.R. Allmaras. 1997. Comments on the Feasibility of LES for Wings, and on a Hybrid RANS/LES Approach," 1st AFOSR Int. Conf. on DNS/LES. In: *Advances in DNS/LES*, C. Liu and Z. Liu (Eds.), Greyden Press, Columbus, OH.
- [9] Shur M., P. Spalart., M. Strelets, A. Travin. 1996. Navier-Stokes Simulation of Shedding Turbulent Flow past a Circular Cylinder and a Cylinder with Backward Splitter Plate. In: *3rd ECCOMAS Computational Fluid Dynamics Conference.* 676–682.
- [10] Spalart P.R. 2001. Young Person Guide to Detached Eddy Simulation Grids. NASA/CR-2001-211032.
- [11] Shur M., M. Strelets, A. Travin. 2004. High-Order Implicit Multi-Block Navier-Stokes Code: Ten-Year Experience of Application to RANS/DES/LES/DNS of Turbulence In: *Proceedings of the 7th Symposium on Overset Composite Grid and Solution Technology, Huntington Beach, California.*
- [12] Roe, P.L. 1981. Approximate Riemann Solvers, Parametric Vectors and Difference Schemes. *J. Comput. Phys.* 43: 357–372.
- [13] Garbaruk, A., M. Shur, M. Strelets, and A. Travin. 2008. Supersonic Base Flow. In: *A European Effort on Hybrid RANS-LES Modelling. Notes on Numerical Fluid Mechanics and Multidisciplinary Design.* 103:197-206.
- [14] Lüdeke, H., V. Togiti. 2006. Detached Eddy Simulation of Supersonic Shear Layer Wake Flows. In: *Int. Conference on Boundary and Interior Layers, Göttingen, Germany.*